Chinese Journal of Aeronautics, (2014),27(2): 375–382

Chinese Society of Aeronautics and Astronautics
& Beihang University

Chinese Journal of Aeronautics

cja@buaa.edu.cn
www.sciencedirect.com

Adaptive finite-time backstepping control for attitude tracking of spacecraft based on rotation matrix

Guo Yong, Song Shenmin *

Center for Control Theory and Guidance Technology, Harbin Institute of Technology, Harbin 150001, China

Received 16 April 2013; revised 2 July 2013; accepted 4 November 2013
Available online 1 March 2014

KEYWORDS

Adaptive control;
Attitude control;
Backstepping;
Finite-time control;
Robustness

Abstract This paper investigates two finite-time controllers for attitude control of spacecraft based on rotation matrix by an adaptive backstepping method. Rotation matrix can overcome the drawbacks of unwinding which makes a spacecraft perform a large-angle maneuver when a small-angle maneuver in the opposite rotational direction is sufficient to achieve the objective. With the use of adaptive control, the first robust finite-time controller is continuous without a chattering phenomenon. The second robust finite-time controller can compensate external disturbances with unknown bounds. Theoretical analysis shows that both controllers can make a spacecraft following a time-varying reference attitude signal in finite time and guarantee the stability of the overall closed-loop system. Numerical simulations are presented to demonstrate the effectiveness of the proposed control schemes.

1. Introduction

Attitude control of spacecraft has received lots of research interest, and a number of research works have been reported. A survey of attitude representations, such as unit quaternion, Rodrigues parameters (RPs), modified Rodrigues parameters (MRPs), etc., have been investigated.[1–3] However, unit quaternion and MRPs are unable to represent the set of attitudes both globally and uniquely that can result in undesirable behaviors such as unwinding.[4,5] Unwinding may result in fuel consumption by traveling a long distance before returning to a desired attitude when a closed-loop system is close to a desired attitude equilibrium.[4] In order to deal with the problem, rotation matrix that represents the set of attitudes both globally and uniquely has received lots of research interest during the last decades.[6–9] Lee[10] proposed an attitude controller by a new attitude error function for an attitude tracking control system on SO(3) (3-dimentional special orthogonal group) to deal with large-angle rotational maneuvers. Weiss and Cruz gave the robust controllers that require no knowledge of the mass distribution of the spacecraft, respectively.[11,12] These attitude parameters were applied in attitude control with various controllers to acquire the results of asymptotical and exponential stabilities of the spacecraft attitude tracking system by using Lyapunov's theorems, Matrosov's theorem, and Barbalat's lemma.

However, asymptotic and exponential stabilities imply that the spacecraft attitude tracking system converges to the equilibrium as time going to infinity. Therefore, the finite-time stabilization of dynamical systems leads to wide applications in

* Corresponding author. Tel.: +86 451 86402204 8212.
E-mail address: songshenmin@hit.edu.cn (S. Song).

☆ Peer review under responsibility of Editorial Committee of CJA.

Production and hosting by Elsevier

1000-9361 © 2014 Production and hosting by Elsevier Ltd. on behalf of CSAA & BUAA. Open access under CC BY-NC-ND license.
http://dx.doi.org/10.1016/j.cja.2014.02.017

attitude tracking of spacecraft. A general framework for finite-time stability analysis of nonlinear dynamical systems was developed by Lyapunov functions[13] and there are many methods to design controllers.

Firstly, finite-time control laws are often sought from the class of homogeneous functions.[14–17] Finite-time control of robot systems was studied through both state feedback and dynamic output feedback control.[14] Bhat and Bernstein[15] gave a class of bounded continuous time-invariant finite-time stabilizing feedback laws for the double integrator. Meng et al.[16] proposed distributed attitude containment control laws for multiple rigid bodies with multiple stationary and dynamic leaders. Du and Li[17] investigated the global finite-time attitude stabilization problem for a rigid spacecraft system. However, it only dealt with the attitude regulator problem of the spacecraft to design a finite-time controller by a homogeneous method.

Secondly, terminal sliding mode control (TSMC) is considered to be a finite-time control scheme. Yu et al.[18] proposed a continuous finite-time control scheme with TSMC for rigid robotic manipulators. Wu et al.[19] investigated two robust sliding mode controllers based on the quaternion to solve the spacecraft attitude tracking control problem. Wang et al.[20] investigated a TSMC law to make the defined dynamical synchronization error converging to the desired trajectory in finite time by using the dual-quaternion representation.

Finally, we can also provide a finite-time controller by a backstepping method based on Lyapunov functions. Reichhartinger and Horn[21] investigated a control law based on the ideas of backstepping. Zhang and Duan[22] proposed a robust finite-time control strategy to enable a spacecraft to track a reference position and rotation motions in finite time. Liu et al.[23] proposed robust control for attitude tracking of spacecraft based on the backstepping method.

None of the aforementioned approaches can provide finite-time control to suppress unknown bounds of external disturbances for a spacecraft based on rotation matrix. To overcome these drawbacks, we investigate robust finite-time control to solve the spacecraft attitude tracking control problem. Compared with the listed literatures, the contributions are as follows. (1) Finite-time stability of the tracking system based on rotation matrix is guaranteed by a Lyapunov-based approach. (2) The continuous controller is robust to external disturbances with bounds and without chattering. (3) By virtue of the novel use of adaptive control, the discontinuous controller is robust to time-varying external disturbances with unknown bounds.

This paper is organized as follows. An attitude dynamic model is established in the following section. In Section 3, firstly, a state error is given, and then two controllers are proposed. Furthermore, the corresponding stability proofs are given as well. Numerical simulations are presented in Section 4. The paper is closed with some concluding remarks.

2. Spacecraft attitude dynamics

Quaternion is often used in attitude control to represent a rigid-body attitude. However, as a physical attitude $\boldsymbol{R} \in \mathrm{SO}(3)$ is represented by a pair of quaternion, unwinding can occur in the continuous controller designed by quaternion.[4] Unwinding has been rigorously analyzed in Refs. 4,5, and from Ref. 4, we can get that controllers based on rotation matrix can deal with the problem.

We employ rotation matrix to describe the attitudes of a spacecraft to avoid ambiguities and singularities. Specifically, the attitude dynamics of the spacecraft is given by Eq. (1) and Eq. (2). Here, $\boldsymbol{\omega} \in \mathbf{R}^{3\times1}$ is the angular velocity of the spacecraft in the body frame. $\boldsymbol{d} \in \mathbf{R}^{3\times1}$ and $\boldsymbol{u} \in \mathbf{R}^{3\times1}$ are the external disturbance torque and control torque, respectively. $\boldsymbol{J} \in \mathbf{R}^{3\times3}$ denotes the inertia matrix. $\boldsymbol{R} \in \mathrm{SO}(3)$ (3-dimentional special orthogonal group) is the rotation matrix that transforms the body frame into the inertial frame resolved in the body frame. $\boldsymbol{\omega}^{\times}$ is the skew-symmetric matrix and the cross-product operation $\times$ transforms a vector in $\mathbf{R}^{3\times1}$ to a skew-symmetric matrix.

$$\dot{\boldsymbol{R}} = \boldsymbol{R}\boldsymbol{\omega}^{\times} \tag{1}$$

$$\boldsymbol{J}\dot{\boldsymbol{\omega}} = -\boldsymbol{\omega}^{\times}\boldsymbol{J}\boldsymbol{\omega} + \boldsymbol{u} + \boldsymbol{d} \tag{2}$$

$$\boldsymbol{\omega}^{\times} = \begin{bmatrix} 0 & -\omega_3 & \omega_2 \\ \omega_3 & 0 & -\omega_1 \\ -\omega_2 & \omega_1 & 0 \end{bmatrix} \tag{3}$$

$\tilde{\boldsymbol{R}}$ is the error rotation matrix defined in Eq. (4). $\tilde{\boldsymbol{\omega}}$ is the angular velocity error resolved in the body frame defined in Eq. (5). $\boldsymbol{R}_{\mathrm{d}} \in \mathrm{SO}(3)$ is a given smooth reference attitude and $\boldsymbol{\omega}_{\mathrm{d}} \in \mathbf{R}^{3\times1}$ is the reference angular velocity with respect to the inertial frame resolved in the reference frame.

$$\tilde{\boldsymbol{R}} = \boldsymbol{R}_{\mathrm{d}}^{\mathrm{T}}\boldsymbol{R} \tag{4}$$

$$\tilde{\boldsymbol{\omega}} = \boldsymbol{\omega} - \tilde{\boldsymbol{R}}^{\mathrm{T}}\boldsymbol{\omega}_{\mathrm{d}} \tag{5}$$

In combination with Eqs. (1)–(5), the attitude dynamics of the spacecraft are given by Eq. (6) and Eq. (7).

$$\dot{\tilde{\boldsymbol{R}}} = \tilde{\boldsymbol{R}}\tilde{\boldsymbol{\omega}}^{\times} \tag{6}$$

$$\begin{aligned}\boldsymbol{J}\dot{\tilde{\boldsymbol{\omega}}} = {} & [(\boldsymbol{J}\boldsymbol{\omega})^{\times} - (\tilde{\boldsymbol{R}}^{\mathrm{T}}\boldsymbol{\omega}_{\mathrm{d}})^{\times}\boldsymbol{J} - \boldsymbol{J}(\tilde{\boldsymbol{R}}^{\mathrm{T}}\boldsymbol{\omega}_{\mathrm{d}})^{\times}]\tilde{\boldsymbol{\omega}} \\ & - (\tilde{\boldsymbol{R}}^{\mathrm{T}}\boldsymbol{\omega}_{\mathrm{d}})^{\times}\boldsymbol{J}\tilde{\boldsymbol{R}}^{\mathrm{T}}\boldsymbol{\omega}_{\mathrm{d}} - \boldsymbol{J}\tilde{\boldsymbol{R}}^{\mathrm{T}}\dot{\boldsymbol{\omega}}_{\mathrm{d}} + \boldsymbol{u} + \boldsymbol{d}\end{aligned} \tag{7}$$

3. Design of the controller

3.1. State error

One of the most difficult problems in the attitude control based on rotation matrix is to choose a suitable error. We almost can't use the error rotation matrix $\tilde{\boldsymbol{R}}$ to design the controller. Many kinds of errors are constructed during the last decade, but they are not convenient to use. A new attitude error function was constructed and some interesting features of the attitude error function were demonstrated in Ref. 10. The attitude error function $\psi(\tilde{\boldsymbol{R}})$ and error vector $\boldsymbol{e}_{\tilde{R}}$ were defined in Eq. (8) and Eq. (9). Here, $-1 \leqslant \mathrm{tr}(\tilde{\boldsymbol{R}}) \leqslant 3$, and the map $\vee$ denotes the inverse of the cross-product operation which transforms a skew-symmetric matrix to a vector. For example, $(\boldsymbol{a}^{\times})^{\vee} = \boldsymbol{a}$ and$(\boldsymbol{A}^{\vee})^{\times} = \boldsymbol{A}$, where $\boldsymbol{a} \in \mathbf{R}^{3\times1}$ and $\boldsymbol{A}$ is a skew-symmetric matrix.

$$\psi(\tilde{\boldsymbol{R}}) = 2 - \sqrt{1 + \mathrm{tr}(\tilde{\boldsymbol{R}})} \tag{8}$$

$$\boldsymbol{e}_{\tilde{R}} = \frac{1}{2\sqrt{1 + \mathrm{tr}(\tilde{\boldsymbol{R}})}}(\tilde{\boldsymbol{R}} - \tilde{\boldsymbol{R}}^{\mathrm{T}})^{\vee} \tag{9}$$

Applying the new attitude error function defined by Eqs. (8) and (9), we can rewrite Eqs. (6) and (7) as Eqs. (10)–(12)

$$\dot{\boldsymbol{e}}_{\widetilde{\boldsymbol{R}}} = \boldsymbol{E}\tilde{\boldsymbol{\omega}} \tag{10}$$

$$\boldsymbol{J}\dot{\tilde{\boldsymbol{\omega}}} = \left\{(\boldsymbol{J}\boldsymbol{\omega})^{\times} - (\widetilde{\boldsymbol{R}}^{\mathrm{T}}\boldsymbol{\omega}_{\mathrm{d}})^{\times}\boldsymbol{J} - \boldsymbol{J}(\widetilde{\boldsymbol{R}}^{\mathrm{T}}\boldsymbol{\omega}_{\mathrm{d}})^{\times}\right\}\tilde{\boldsymbol{\omega}} - (\widetilde{\boldsymbol{R}}^{\mathrm{T}}\boldsymbol{\omega}_{\mathrm{d}})^{\times}\boldsymbol{J}\widetilde{\boldsymbol{R}}^{\mathrm{T}}\boldsymbol{\omega}_{\mathrm{d}} - \boldsymbol{J}\widetilde{\boldsymbol{R}}^{\mathrm{T}}\dot{\boldsymbol{\omega}}_{\mathrm{d}} + \boldsymbol{u} + \boldsymbol{d} \tag{11}$$

$$\boldsymbol{E} = \frac{1}{2\sqrt{1+\mathrm{tr}(\widetilde{\boldsymbol{R}})}}(\mathrm{tr}(\widetilde{\boldsymbol{R}})\mathbf{I} - \widetilde{\boldsymbol{R}}^{\mathrm{T}} + 2\boldsymbol{e}_{\widetilde{\boldsymbol{R}}}\boldsymbol{e}_{\widetilde{\boldsymbol{R}}}^{\mathrm{T}}) \tag{12}$$

Note that Eqs. (10) and (12) are valid only if $\boldsymbol{E}$ is nonsingular, which indicates that the case $\mathrm{tr}(\widetilde{\boldsymbol{R}}) = -1$ does not occur. The attitude error vector $\boldsymbol{e}_{\widetilde{\boldsymbol{R}}}$ and $\boldsymbol{E}$ are well defined in the set $\upsilon = \{\boldsymbol{R} \in \mathrm{SO}(3) | \psi(\widetilde{\boldsymbol{R}}) < 2\}$. The following lemmas are useful to design the attitude control of the spacecraft.

Lemma 1. [10] *In* υ, $\psi(\widetilde{\boldsymbol{R}})$ *is locally quadratic.*

$$\|\boldsymbol{e}_{\widetilde{\boldsymbol{R}}}\|^2 \leqslant \psi(\widetilde{\boldsymbol{R}}) \leqslant 2\|\boldsymbol{e}_{\widetilde{\boldsymbol{R}}}\|^2 \tag{13}$$

Lemma 2. [10] *Let* $\mathbf{R}_d^{\mathrm{T}}\mathbf{R} = exp(\boldsymbol{x}^{\times})$, *and there exists* $\boldsymbol{x} \in \mathbf{R}^{3\times 1}$, *with* $\|\boldsymbol{x}\| \leqslant \pi$. *Eigenvalues of* $\boldsymbol{E}^{\mathrm{T}}\boldsymbol{E}$ *are given by* $\frac{1}{4}, \frac{1}{4}, \frac{1}{8}(1+\cos\|\boldsymbol{x}\|)$. *It follows that the matrix 2-norm of* $\boldsymbol{E}$ *is* $\|\boldsymbol{E}\| = \frac{1}{2}$. *We can also get that* $\|\boldsymbol{e}_{\widetilde{\boldsymbol{R}}}\|^2 = 4\sin^2\frac{\|\boldsymbol{x}\|}{4}\cos^2\frac{\|\boldsymbol{x}\|}{4}$ *and* $\psi(\widetilde{\boldsymbol{R}}) = 4\sin^2\frac{\|\boldsymbol{x}\|}{4}$.

Lemma 3. [10] *In* υ, $\|x\| \neq \pi$, *so* $\boldsymbol{E}$ *is an invertible matrix and* $\|\boldsymbol{e}_{\widetilde{\boldsymbol{R}}}\| < 1$.

Lemma 4. [18] *Suppose* $\alpha_1, \alpha_2, \cdots, \alpha_n$ *and* $0 < \rho < 2$ *are all positive numbers; then the following inequality holds:*

$$\left(\alpha_1^2 + \alpha_2^2 + \cdots + \alpha_n^2\right)^{\rho} \leqslant \left(\alpha_1^{\rho} + \alpha_2^{\rho} + \cdots + \alpha_n^{\rho}\right)^2 \tag{14}$$

Lemma 5. [18] *Suppose* $\dot{v}(t) \leqslant -\alpha v(t) - \beta v(t)^{\gamma}$, $\forall t_1 \geqslant t_0$, *where* $\alpha > 0, \beta > 0, 0 < \gamma < 1$ *and* $v(t)$ *is a continuous positive definite function. Then the system converges to the equilibrium point in finite time.*

$$t_1 \leqslant t_0 + \frac{1}{\alpha(1-\gamma)}\ln\frac{\alpha v(t_0)^{1-\gamma} + \beta}{\beta} \tag{15}$$

Remark 1. From Lemma 1, Lemma 2, and Eq. (8), we can know that $\psi(\widetilde{\boldsymbol{R}}) = 2$ is equivalent to $\widetilde{\boldsymbol{R}} \notin \upsilon$ and $\|\boldsymbol{E}^{-1}\| = \sqrt{8/(1+\cos(2\arcsin(\|\boldsymbol{e}_{\widetilde{\boldsymbol{R}}}\|)))}$. $\|\boldsymbol{x}\| = \pi$ and $\|\boldsymbol{e}_{\widetilde{\boldsymbol{R}}}\| = 1$ are all equivalent to $\psi(\widetilde{\boldsymbol{R}}) = 2$.

3.2. Controller design

Motivated by Ref. 10, we employ the idea of finite-time control to design a robust controller for the attitude control of the spacecraft based on rotation matrix. As Eqs. (10) and (11) constitute a standard cascade system, we apply the backstepping method to design a control scheme. The variables $\boldsymbol{x}_1$ and $\boldsymbol{x}_2$ are defined in Eqs. (16) and (17).

$$\boldsymbol{x}_1 = \boldsymbol{e}_{\widetilde{\boldsymbol{R}}} \tag{16}$$

$$\boldsymbol{x}_2 = \tilde{\boldsymbol{\omega}} - \tilde{\boldsymbol{\omega}}^{v} \tag{17}$$

In combination with Eqs. (11) and (17), we can get Eq. (18).

$$\dot{\boldsymbol{x}}_2 = \boldsymbol{J}^{-1}\left\{[(\boldsymbol{J}\boldsymbol{\omega})^{\times} - (\widetilde{\boldsymbol{R}}^{\mathrm{T}}\boldsymbol{\omega}_{\mathrm{d}})^{\times}\boldsymbol{J} - \boldsymbol{J}(\widetilde{\boldsymbol{R}}^{\mathrm{T}}\boldsymbol{\omega}_{\mathrm{d}})^{\times}]\tilde{\boldsymbol{\omega}} - (\widetilde{\boldsymbol{R}}^{\mathrm{T}}\boldsymbol{\omega}_{\mathrm{d}})^{\times}\boldsymbol{J}\widetilde{\boldsymbol{R}}^{\mathrm{T}}\boldsymbol{\omega}_{\mathrm{d}} - \boldsymbol{J}\widetilde{\boldsymbol{R}}^{\mathrm{T}}\dot{\boldsymbol{\omega}}_{\mathrm{d}} - \boldsymbol{J}\dot{\tilde{\boldsymbol{\omega}}}^{v} + \boldsymbol{u} + \boldsymbol{d}\right\} \tag{18}$$

In the light of Eq. (10), the desired finite-time control is firstly designed as Eq. (19). Here, k_1,k_2 and η are positive constants. $0 < \gamma < 1$, $f(\boldsymbol{x}_1) = [f(x_{1,1})\ f(x_{1,2})\ f(x_{1,3})]^{\mathrm{T}}$, $\mathrm{sig}(x_{1,i})^{\gamma} = \mathrm{sign}(x_{1,i})|x_{1,i}|^{\gamma}$, $r_1 = (2-\gamma)\eta^{\gamma-1}$, $r_2 = (\gamma-1)\eta^{\gamma-2}$.

$$\tilde{\boldsymbol{\omega}}^{v} = -k_1\boldsymbol{E}^{-1}\boldsymbol{x}_1 - k_2\boldsymbol{E}^{-1}f(\boldsymbol{x}_1) \tag{19}$$

$$f(x_{1,i}) = \begin{cases} r_1 x_{1,i} + r_2\ \mathrm{sign}(x_{1,i})x_{1,i}^2 & |x_{1,i}| \leqslant \eta, \quad i = 1,2,3 \\ \mathrm{sig}(x_{1,i})^{\gamma} & \text{Others} \end{cases} \tag{20}$$

Proposition 1. *For Eq. (10), if the virtual angular velocity is designed as Eq. (19) when* $\boldsymbol{\omega}_{\mathrm{d}}$ *and* $\dot{\boldsymbol{\omega}}_{\mathrm{d}}$ *are all bounded, we can conclude that* $x_{1,i}, i = 1,2,3$ *converges to* $|x_{1,i}| \leqslant \eta$ *in finite time.*

Proof 1. We choose the Lyapunov function as $V_{1,i} = \frac{1}{2}x_{1,i}^2$. By applying Eq. (10) and Eq. (19), the derivative of $V_{1,i}, i = 1,2,3$ can be written as

$$\dot{V}_{1,i} = x_{1,i}\dot{x}_{1,i} = -k_1x_{1,i}^2 - k_2x_{1,i}f(x_{1,i}).$$

When $|x_{1,i}| > \eta$, $\dot{V}_{1,i}$ can be written as

$$\dot{V}_{1,i} = -k_1x_{1,i}^2 - k_2x_{1,i}\mathrm{sig}(x_{1,i})^{\gamma} \leqslant -2k_1V_{1,i} - 2^{(\gamma+1)/2}k_2V_{1,i}^{(\gamma+1)/2}.$$

When $|x_{1,i}| \leqslant \eta$, $\dot{V}_{1,i}$ can be written as

$$\dot{V}_{1,i} = -k_1x_{1,i}^2 - k_2r_1x_{1,i}^2 - k_2r_2\ \mathrm{sign}(x_{1,i})x_{1,i}^2 \leqslant -2k_1V_{1,i}.$$

By using Lemma 4, $x_{1,i}$ will converge to $|x_{1,i}| \leqslant \eta$ in finite time.

Based on the backstepping method, the control law for the spacecraft is given by Eqs. (21)–(23). $\hat{\boldsymbol{d}}$ is the estimation values of $\boldsymbol{d}$. $\boldsymbol{Q}$ is a positive definite diagonal matrix. k_3,k_4 and β are positive constants.

$$\boldsymbol{u} = -\left\{(\boldsymbol{J}\boldsymbol{\omega})^{\times} - (\widetilde{\boldsymbol{R}}^{\mathrm{T}}\boldsymbol{\omega}_{\mathrm{d}})^{\times}\boldsymbol{J} - \boldsymbol{J}(\widetilde{\boldsymbol{R}}^{\mathrm{T}}\boldsymbol{\omega}_{\mathrm{d}})^{\times}\right\}\tilde{\boldsymbol{\omega}} + (\widetilde{\boldsymbol{R}}^{\mathrm{T}}\boldsymbol{\omega}_{\mathrm{d}})^{\times}\boldsymbol{J}\widetilde{\boldsymbol{R}}^{\mathrm{T}}\boldsymbol{\omega}_{\mathrm{d}} + \boldsymbol{J}\widetilde{\boldsymbol{R}}^{\mathrm{T}}\dot{\boldsymbol{\omega}}_{\mathrm{d}} + \boldsymbol{J}\dot{\tilde{\boldsymbol{\omega}}}^{v} - \hat{\boldsymbol{d}} - k_3\boldsymbol{J}\boldsymbol{x}_2 - k_4\boldsymbol{J}\,\mathrm{sig}(\boldsymbol{x}_2)^{\gamma} - \beta\boldsymbol{J}\boldsymbol{E}^{\mathrm{T}}\boldsymbol{x}_1 \tag{21}$$

$$\dot{\hat{\boldsymbol{d}}} = \frac{1}{\beta}\boldsymbol{Q}\boldsymbol{J}^{-\mathrm{T}}\boldsymbol{x}_2 \tag{22}$$

$$\mathrm{sig}\ (\boldsymbol{x}_2)^{\gamma} = [|x_{2,1}|^{\gamma}\ \mathrm{sign}(x_{2,1})|x_{2,2}|^{\gamma}\ \mathrm{sign}(x_{2,2})|x_{2,3}|^{\gamma}\ \mathrm{sign}(x_{2,3})]^{\mathrm{T}} \tag{23}$$

□

Theorem 1. *Using Eqs. (21)–(23) for the system Eqs. (10) and (11), when* $\boldsymbol{\omega}_{\mathrm{d}}$ *and* $\dot{\boldsymbol{\omega}}_{\mathrm{d}}$ *are all bounded and d is constant, we conclude that* x_1,x_2, *and* $\tilde{\boldsymbol{d}}$ *are all bounded.*

$$V_2 = \frac{1}{2}\boldsymbol{x}_1^{\mathrm{T}}\boldsymbol{x}_1 + \frac{1}{2\beta}\boldsymbol{x}_2^{\mathrm{T}}\boldsymbol{x}_2 + \frac{1}{2}\tilde{\boldsymbol{d}}^{\mathrm{T}}\boldsymbol{Q}^{-1}\tilde{\boldsymbol{d}} \tag{24}$$

Proof 2. We choose the Lyapunov function V_2 as Eq. (24), where $\tilde{\boldsymbol{d}} = \boldsymbol{d} - \hat{\boldsymbol{d}}$. Applying Eq. (18) and Eqs. (21)–(23), the derivative of V_2 can be written as:

$$\begin{aligned}\dot{V}_2 &= \boldsymbol{x}_1^{\mathrm{T}}\dot{\boldsymbol{x}}_1 + \frac{1}{\beta}\boldsymbol{x}_2^{\mathrm{T}}\dot{\boldsymbol{x}}_2 - \tilde{\boldsymbol{d}}^{\mathrm{T}}\boldsymbol{Q}^{-1}\dot{\tilde{\boldsymbol{d}}} \\ &= -k_1\boldsymbol{x}_1^{\mathrm{T}}\boldsymbol{x}_1 - k_2\boldsymbol{x}_1^{\mathrm{T}}f(\boldsymbol{x}_1) + \frac{1}{\beta}\boldsymbol{x}_2^{\mathrm{T}}\boldsymbol{J}^{-1}\tilde{\boldsymbol{d}} - \frac{k_3}{\beta}\boldsymbol{x}_2^{\mathrm{T}}\boldsymbol{x}_2 \\ &\quad - \frac{k_4}{\beta}\boldsymbol{x}_2^{\mathrm{T}}\mathrm{sig}(\boldsymbol{x}_2)^{\gamma} - \tilde{\boldsymbol{d}}^{\mathrm{T}}\boldsymbol{Q}^{-1}\dot{\tilde{\boldsymbol{d}}} \\ &= -k_1\boldsymbol{x}_1^{\mathrm{T}}\boldsymbol{x}_1 - k_2\boldsymbol{x}_1^{\mathrm{T}}f(\boldsymbol{x}_1) - \frac{k_3}{\beta}\boldsymbol{x}_2^{\mathrm{T}}\boldsymbol{x}_2 - \frac{k_4}{\beta}\boldsymbol{x}_2^{\mathrm{T}}\ \mathrm{sig}(\boldsymbol{x}_2)^{\gamma} \\ &\leqslant 0\end{aligned}$$

It can be seen that $\dot{V}_2 \leqslant 0$. Thus V_2 is bound. Therefore, it can be concluded that variables $\boldsymbol{x}_1$, $\boldsymbol{x}_2$, and $\tilde{\boldsymbol{d}}$ are all bounded. Combined with Eqs. (16)–(19), it can be seen that $\tilde{\boldsymbol{\omega}}$ is also bounded. □

Remark 2. In Theorem 1, $\tilde{\boldsymbol{d}}$ does not converge to the regions near zero in finite time. It just guarantees that $\tilde{\boldsymbol{d}}$ has the bound. In Theorem 2, x_1, x_2, and $\tilde{\boldsymbol{\omega}}$ converge to the regions near zero in finite time. In order to facilitate the analysis of finite-time stability in Theorem 2, let $\boldsymbol{\xi} = \frac{1}{\beta}\boldsymbol{J}^{-1}\tilde{\boldsymbol{d}}$ and ξ_{M} is the maximum element of $\|\xi\|$.

Theorem 2. *Consider a spacecraft described by Eq. (18), and the control laws are provided by Eqs. (21)–(23). When ω_d and $\dot{\boldsymbol{\omega}}_{\mathrm{d}}$ are all bounded and d is constant, we can conclude as follows:*

(1) $x_{1,i}$ and $x_{2,i}$ converge to the regions $|x_{1,i}| \leqslant \Delta_1$ and $|x_{2,i}| \leqslant \Delta_2$ in time T. $T \leqslant \max\{t_1,t_2,t_3,t_4\}$. Here, $c_2 = \xi_M^2/4c_1$, in which c_1 is a small positive constant.

$$t_1 \leqslant \frac{1}{\eta_1(1-\gamma)}\ln\frac{\eta_1 V_3(t_0)^{1-\gamma}+\eta_2}{\eta_2},$$

$$t_2 \leqslant \frac{1}{\mu_1(1-\gamma)}\ln\frac{\mu_1 V_3(t_0)^{1-\gamma}+\mu_2}{\mu_2} \tag{25}$$

$$t_3 \leqslant \frac{1}{\delta_1(1-\gamma)}\ln\frac{\delta_1 V_3(t_0)^{1-\gamma}+\delta_2}{\delta_2},$$

$$t_4 \leqslant \frac{1}{\varphi_1(1-\gamma)}\ln\frac{\varphi_1 V_3(t_0)^{1-\gamma}+\varphi_2}{\varphi_2} \tag{26}$$

$$\Delta_1 = \max\left\{\eta, \min\left(\left(\frac{c_2}{k_1}\right)^{1/2}, \left(\frac{c_2}{k_2}\right)^{1/1+\gamma}\right)\right\} \tag{27}$$

$$\Delta_2 = \min\left\{\left(\frac{c_2\beta}{k_3-c_1\beta}\right)^{1/2}, \left(\frac{\beta c_2}{k_4}\right)^{1/1+\gamma}\right\} \tag{28}$$

(2) The errors $\tilde{\boldsymbol{\omega}}$ converge to the regions $\|\tilde{\boldsymbol{\omega}}\| \leqslant \Delta_3$ in finite time.

$$\Delta_3 \leqslant \sqrt{3}\Delta_2 + k_1\sqrt{\frac{8}{1+\cos\left(\arcsin\left(\sqrt{3}\Delta_1\right)\right)}}\sqrt{3}\Delta_1 + k_2 \times \sqrt{\frac{8}{1+\cos\left(\arcsin\left(\sqrt{3}\Delta_1\right)\right)}}\left(\sqrt{3}\Delta_1\right)^{\gamma} \tag{29}$$

(3) The region of attraction is given by $\boldsymbol{x}_1^{\mathrm{T}}(0)\boldsymbol{x}_1(0) + \frac{1}{\beta}\boldsymbol{x}_2^{\mathrm{T}}(0)\boldsymbol{x}_2(0) + \tilde{\boldsymbol{d}}^{\mathrm{T}}(0)\boldsymbol{Q}^{-1}\tilde{\boldsymbol{d}}(0) < 1$. Here, $G(0)$ is the initial value of G.

Proof 3. We choose the Lyapunov function as $V_{3,i} = \frac{1}{2}x_{1,i}^2 + \frac{1}{2\beta}x_{2,i}^2, i = 1,2,3$. When $|x_{1,i}| > \eta$, applying Eq. (18) and Eqs. (21)–(23), the derivative of $V_{3,i}$ can be written as

$$\begin{aligned}\dot{V}_{3,i} &= x_{1,i}\dot{x}_{1,i} + \frac{1}{\beta}x_{2,i}\dot{x}_{2,i} \\ &= -k_1x_{1,i}^2 - k_2x_{1,i}\,\mathrm{sig}(x_{1,i})^{\gamma} - \frac{k_3}{\beta}x_{2,i}^2 - \frac{k_4}{\beta}x_{2,i}\,\mathrm{sig}(x_{2,i})^{\gamma} + x_{2,i}\xi_i \\ &\leqslant -k_1x_{1,i}^2 - k_2x_{1,i}\,\mathrm{sig}(x_{1,i})^{\gamma} - \frac{k_3}{\beta}x_{2,i}^2 - \frac{k_4}{\beta}x_{2,i}\,\mathrm{sig}(x_{2,i})^{\gamma} + |x_{2,i}|\xi_M \\ &\leqslant -k_1x_{1,i}^2 - k_2x_{1,i}\,\mathrm{sig}(x_{1,i})^{\gamma} - \left(\frac{k_3}{\beta}-c_1\right)x_{2,i}^2 - \frac{k_4}{\beta}x_{2,i}\,\mathrm{sig}(x_{2,i})^{\gamma} + c_2\end{aligned}$$

In order to deal with c_2, $\dot{V}_{3,i}$ can be rewritten as Eqs. (30)–(33). We will discuss these situations in Cases 1–4.

$$\dot{V}_{3,i} \leqslant -\left(k_1 - \frac{c_2}{x_{1,i}^2}\right)x_{1,i}^2 - k_2x_{1,i}\ \mathrm{sig}(x_{1,i})^{\gamma} - \left(\frac{k_3}{\beta}-c_1\right)x_{2,i}^2 - \frac{k_4}{\beta}x_{2,i}\ \mathrm{sig}(x_{2,i})^{\gamma} \tag{30}$$

$$\dot{V}_{3,i} \leqslant -k_1x_{1,i}^2 - \left(k_2 - \frac{c_2}{x_{1,i}\mathrm{sig}(x_{1,i})^{\gamma}}\right)x_{1,i}\ \mathrm{sig}(x_{1,i})^{\gamma} - \left(\frac{k_3}{\beta}-c_1\right)x_{2,i}^2 - \frac{k_4}{\beta}x_{2,i}\ \mathrm{sig}(x_{2,i})^{\gamma} \tag{31}$$

$$\dot{V}_{3,i} \leqslant -k_1x_{1,i}^2 - k_2x_{1,i}\ \mathrm{sig}(x_{1,i})^{\gamma} - \left(\frac{k_3}{\beta}-c_1-\frac{c_2}{x_{2,i}^2}\right)x_{2,i}^2 - \frac{k_4}{\beta}x_{2,i}\ \mathrm{sig}(x_{2,i})^{\gamma} \tag{32}$$

$$\dot{V}_{3,i} \leqslant -k_1x_{1,i}^2 - k_2x_{1,i}\ \mathrm{sig}(x_{1,i})^{\gamma} - \left(\frac{k_3}{\beta}-c_1\right)x_{2,i}^2 - \left(\frac{k_4}{\beta}-\frac{c_2}{x_{2,i}\ \mathrm{sig}(x_{2,i})^{\gamma}}\right)x_{2,i}\ \mathrm{sig}(x_{2,i})^{\gamma} \tag{33}$$

□

Case 1. Assuming $\eta_1 = 2\min\left\{k_1 - \frac{c_2}{x_{1,i}^2}, k_3 - c_1\beta\right\}$ and $\eta_2 = 2^{(\gamma+1)/2}\min\{k_2, k_4\beta^{(\gamma-1)/2}\}$, Eq. (30) can be rewritten as:

$$\begin{aligned}\dot{V}_{3,i} &\leqslant -\left(k_1 - \tfrac{c_2}{x_{1,i}^2}\right)x_{1,i}^2 - \frac{1}{\beta}(k_3-c_1\beta)x_{2,i}^2 - k_2(x_{1,i}^2)^{(\gamma+1)/2} \\ &\quad -k_4\beta^{(\gamma-1)/2}\left(\frac{1}{\beta}x_{2,i}^2\right)^{(\gamma+1)/2} \\ &\leqslant -\frac{1}{2}\eta_1\left(x_{1,i}^2+\frac{1}{\beta}x_{2,i}^2\right) - 2^{-(\gamma+1)/2}\eta_2\left(\left(x_{1,i}^2\right)^{(\gamma+1)/2} + \left(\frac{1}{\beta}x_{2,i}^2\right)^{(\gamma+1)/2}\right) \\ &\leqslant -\frac{1}{2}\eta_1\left(x_{1,i}^2+\frac{1}{\beta}x_{2,i}^2\right) - 2^{-(\gamma+1)/2}\eta_2\left(x_{1,i}^2+\frac{1}{\beta}x_{2,i}^2\right)^{(\gamma+1)/2} \\ &\leqslant -\eta_1V_{3,i} - \eta_2V_{3,i}^{(\gamma+1)/2}\end{aligned}$$

We can obtain that, if $\eta_1 > 0$, $\eta_2 > 0$, $x_{1,i}$ will converge to the region $|x_{1,i}| \leqslant \left(\frac{c_2}{k_1}\right)^{1/2}$ in finite time and $x_{2,i}$ will converge to zero in finite time. By using Lemma 5, we can get that $x_{1,i}$ and $x_{2,i}$ converge to the region in time $t_1 \leqslant \frac{1}{\eta_1(1-\gamma)}\ln\frac{\eta_1V_3(t_0)^{1-\gamma}+\eta_2}{\eta_2}$.

Case 2. Assuming $\mu_1 = 2\min\{k_1, k_3 - c_1\beta\}$ and $\mu_2 = 2^{(\gamma+1)/2}\min\left\{k_2 - \frac{c_2}{x_{1,i}\ \mathrm{sig}(x_{1,i})^{\gamma}}, k_4\beta^{(\gamma-1)/2}\right\}$ Eq. (31) can be rewritten as:

$$\begin{aligned}\dot{V}_{3,i} &\leqslant -k_1 x_{1,i}^2 - \left(k_2 - \frac{c_2}{x_{1,i}\,\mathrm{sig}(x_{1,i})^{\gamma}}\right)(x_{1,i}^2)^{(\gamma+1)/2} - \left(\frac{k_3}{\beta} - c_1\right)x_{2,i}^2 \\ &\quad - \frac{k_4}{\beta}\left(x_{2,i}^2\right)^{(\gamma+1)/2} \\ &\leqslant -\frac{1}{2}\mu_1\left(x_{1,i}^2 + \frac{1}{\beta}x_{2,i}^2\right) - 2^{-(\gamma+1)/2}\mu_2\left(x_{1,i}^2 + \frac{1}{\beta}x_{2,i}^2\right)^{(\gamma+1)/2} \\ &\leqslant -\mu_1 V_{3,i} - \mu_2 V_{3,i}^{(\gamma+1)/2}\end{aligned}$$

We can obtain that, if $\mu_1 > 0, \mu_2 > 0$, $x_{1,i}$ will converge to the region $|x_{1,i}| \leqslant \left(\frac{c_2}{k_2}\right)^{1/1+\gamma}$ in finite time and $x_{2,i}$ will converge to zero in finite time. By using Lemma 5, we can get that $x_{1,i}$ and $x_{2,i}$ converge to the region in time $t_2 \leqslant \frac{1}{\mu_1(1-\gamma)}\ln\frac{\mu_1 V_3(t_0)^{1-\gamma} + \mu_2}{\mu_2}$.

Case 3. Assuming $\delta_1 = 2\min\left\{k_1, k_3 - c_1\beta - \frac{c_2\beta}{x_{2,i}^2}\right\}$ and $\delta_2 = 2^{(\gamma+1)/2}\min\{k_2, k_4\beta^{(\gamma-1)/2}\}$, Eq. (32) can be rewritten as:

$$\begin{aligned}\dot{V}_{3,i} &\leqslant -k_1 x_{1,i}^2 - k_2\left(x_{1,i}^2\right)^{(\gamma+1)/2} - \left(\tfrac{k_3}{\beta} - c_1 - \frac{c_2}{x_{2,i}^2}\right)x_{2,i}^2 - \frac{k_4}{\beta}(x_{2,i}^2)^{(\gamma+1)/2} \\ &\leqslant -\frac{1}{2}\delta_1\left(x_{1,i}^2 + \frac{1}{\beta}x_{2,i}^2\right) - 2^{-(\gamma+1)/2}\delta_2\left(x_{1,i}^2 + \frac{1}{\beta}x_{2,i}^2\right)^{(\gamma+1)/2} \\ &\leqslant -\delta_1 V_{3,i} - \delta_2 V_{3,i}^{(\gamma+1)/2}\end{aligned}$$

We can obtain that, if $\delta_1 > 0, \delta_2 > 0$, $x_{1,i}$ will converge to zero in finite time and $x_{2,i}$ will converge to the region $|x_{2,i}| \leqslant \left(\frac{c_2\beta}{k_3 - c_1\beta}\right)^{1/2}$ in finite time. By using Lemma 5, we can get that $x_{1,i}$ and $x_{2,i}$ converge to the region in time $t_3 \leqslant \frac{1}{\delta_1(1-\gamma)}\ln\frac{\delta_1 V_3(t_0)^{1-\gamma} + \delta_2}{\delta_2}$.

Case 4. Assuming $\varphi_1 = 2\min\{k_1, k_3 - c_1\beta\}$ and $\varphi_2 = 2^{(\gamma+1)/2}\min\left\{k_2, k_4\beta^{(\gamma-1)/2} - \frac{c_2\beta^{(\gamma+1)/2}}{x_{2,i}\,\mathrm{sig}(x_{2,i})^{\gamma}}\right\}$ Eq. (33) can be rewritten as:

$$\begin{aligned}\dot{V}_{3,i} &\leqslant -k_1 x_{1,i}^2 - k_2\left(x_{1,i}^2\right)^{(\gamma+1)/2} - \left(\frac{k_3}{\beta} - c_1\right)x_{2,i}^2 \\ &\quad - \left(\frac{k_4}{\beta} - \frac{c_2}{x_{2,i}\,\mathrm{sig}(x_{2,i})^{\gamma}}\right)\left(x_{2,i}^2\right)^{(\gamma+1)/2} \\ &\leqslant -\frac{1}{2}\varphi_1\left(x_{1,i}^2 + \frac{1}{\beta}x_{2,i}^2\right) - 2^{-(\gamma+1)/2}\varphi_2\left(x_{1,i}^2 + \frac{1}{\beta}x_{2,i}^2\right)^{(\gamma+1)/2} \\ &\leqslant -\varphi_1 V_{3,i} - \varphi_2 V_{3,i}^{(\gamma+1)/2}\end{aligned}$$

We can obtain that, if $\varphi_1 > 0, \varphi_2 > 0$, $x_{1,i}$ will converge to zero in finite time and $x_{2,i}$ will converge to the region $|x_{2,i}| \leqslant \left(\frac{\beta c_2}{k_4}\right)^{1/1+\gamma}$ in finite time. By using Lemma 5, we can get that $x_{1,i}$ and $x_{2,i}$ converge to the region in time $t_4 \leqslant \frac{1}{\varphi_1(1-\gamma)}\ln\frac{\varphi_1 V_3(t_0)^{1-\gamma} + \varphi_2}{\varphi_2}$. In combination with 1–4, we can get that $x_{1,i}$ and $x_{2,i}$ converge to the regions $|x_{1,i}| \leqslant \Delta_1$ and $|x_{2,i}| \leqslant \Delta_2$ in time $T \leqslant \max\{t_1, t_2, t_3, t_4\}$.

$$|x_{1,i}| \leqslant \Delta_1 = \max\left\{\eta, \min\left(\left(\frac{c_2}{k_1}\right)^{1/2}, \left(\frac{c_2}{k_2}\right)^{1/1+\gamma}\right)\right\} \tag{34}$$

$$|x_{2,i}| \leqslant \Delta_2 = \min\left\{\left(\frac{c_2\beta}{k_3 - c_1\beta_1}\right)^{1/2}, \left(\frac{\beta c_2}{k_4}\right)^{1/1+\gamma}\right\} \tag{35}$$

Now (1) in the Theorem 2 has been proofed.

The stability analysis of $\tilde{\boldsymbol{\omega}}$ convergence to the area near zero is as follows:

$$\tilde{\boldsymbol{\omega}} = \boldsymbol{x}_2 + \tilde{\boldsymbol{\omega}}^{v} \tag{36}$$

$$\tilde{\boldsymbol{\omega}} = \boldsymbol{x}_2 - k_1\boldsymbol{E}^{-1}\boldsymbol{e}_{\tilde{\boldsymbol{R}}} - k_2\boldsymbol{E}^{-1}f(\boldsymbol{x}_1) \tag{37}$$

$$\begin{aligned}\|\tilde{\boldsymbol{\omega}}\| \leqslant \Delta_3 &\leqslant \sqrt{3}\Delta_2 + k_1\sqrt{\frac{8}{1+\cos\left(\arcsin\left(\sqrt{3}\Delta_1\right)\right)}}\sqrt{3}\Delta_1 \\ &\quad + k_2\sqrt{\frac{8}{1+\cos\left(\arcsin\left(\sqrt{3}\Delta_1\right)\right)}}\left(\sqrt{3}\Delta_1\right)^{\gamma}\end{aligned} \tag{38}$$

From Eqs. (35)–(37), we can find that $\tilde{\boldsymbol{\omega}}$ converges to the region $\|\tilde{\boldsymbol{\omega}}\| \leqslant \Delta_3$ in finite time.

Now (2) in the Theorem 2 has been proofed.

In order to keep the attitude error vector $\boldsymbol{e}_{\tilde{\boldsymbol{R}}}$ in the set υ, we keep $\|\boldsymbol{x}_1(0)\|^2 < 1$. From Theorem 1, we can get Eq. (39).

$$\begin{aligned}V_2 &\leqslant V_2(0) \\ &\leqslant \frac{1}{2}\boldsymbol{x}_1^{\mathrm{T}}(0)\boldsymbol{x}_1(0) + \frac{1}{2\beta}\boldsymbol{x}_2^{\mathrm{T}}(0)\boldsymbol{x}_2(0) \\ &\quad + \frac{1}{2}\tilde{\boldsymbol{d}}^{\mathrm{T}}(0)\boldsymbol{Q}^{-1}\tilde{\boldsymbol{d}}(0) < \frac{1}{2}\end{aligned} \tag{39}$$

Further, we can get Eq. (40).

$$\boldsymbol{x}_1^{\mathrm{T}}(0)\boldsymbol{x}_1(0) + \frac{1}{\beta}\boldsymbol{x}_2^{\mathrm{T}}(0)\boldsymbol{x}_2(0) + \tilde{\boldsymbol{d}}^{\mathrm{T}}(0)\boldsymbol{Q}^{-1}\tilde{\boldsymbol{d}}(0) < 1 \tag{40}$$

Now (3) in the Theorem 2 has been proofed.

Remark 3. The robust controller can make the spacecraft following a time-varying reference attitude signal in finite time. Owing to external disturbances, $x_{1,i}$, $x_{2,i}$, and $\tilde{\boldsymbol{\omega}}$ converge to the region near zero in time T.

Remark 4. From Eqs. (27) and (28), it is concluded that the controller parameters k_1 and k_2 determine the accuracy of $x_{1,i}$ and the controller parameters k_3 and k_4 determine the final accuracy of $x_{2,i}$. The smaller $x_{1,i}$ and $x_{2,i}$ are, the bigger k_1, k_2, k_3, and k_4 are required. From Theorem 3, we know that the region of attraction is described by Eq. (40). We can select large β and Q to enlarge the region of attraction.

In Theorem 1 and Theorem 2, it is assumed that $\boldsymbol{d}$ is constant. In order to deal with a time-varying unknown bounded disturbance, we design the discontinuous controller Eqs. (41)–(43). The external disturbance $\boldsymbol{d}$ is assumed to be bounded and satisfy inequality $\|\boldsymbol{d}\| \leqslant d_{\mathrm{M}}$. d_{M} is an unknown positive constant and $\hat{d}_{\mathrm{M}}$ is the estimation values of d_{M}. $\tilde{d}_{\mathrm{M}} = d_{\mathrm{M}} - \hat{d}_{\mathrm{M}}$, χ and λ are positive constants.

$$\begin{aligned}\boldsymbol{u} &= -[(\boldsymbol{J}\boldsymbol{\omega})^{\times} - (\tilde{\boldsymbol{R}}^{\mathrm{T}}\boldsymbol{\omega}_{\mathrm{d}})^{\times}\boldsymbol{J} - \boldsymbol{J}(\tilde{\boldsymbol{R}}^{\mathrm{T}}\boldsymbol{\omega}_{\mathrm{d}})^{\times}]\tilde{\boldsymbol{\omega}} \\ &\quad + (\tilde{\boldsymbol{R}}^{\mathrm{T}}\boldsymbol{\omega}_{\mathrm{d}})^{\times}\boldsymbol{J}\tilde{\boldsymbol{R}}^{\mathrm{T}}\boldsymbol{\omega}_{\mathrm{d}} + \boldsymbol{J}\tilde{\boldsymbol{R}}^{\mathrm{T}}\dot{\boldsymbol{\omega}}_{\mathrm{d}} + \boldsymbol{J}\dot{\tilde{\boldsymbol{\omega}}}^{v} - k_3\boldsymbol{J}\boldsymbol{x}_2 \\ &\quad - k_4\boldsymbol{J}\,\mathrm{sig}(\boldsymbol{x}_2)^{\gamma} - \beta\boldsymbol{J}\boldsymbol{E}^{\mathrm{T}}\boldsymbol{x}_1 - \lambda\boldsymbol{J}\,\mathrm{sign}(\boldsymbol{x}_2) \\ &\quad - \hat{d}_M\,\mathrm{sign}(\boldsymbol{J}^{-\mathrm{T}}\boldsymbol{x}_2)\end{aligned} \tag{41}$$

$$\dot{\hat{d}}_{\mathrm{M}} = \frac{1}{\beta}\chi\left\|\boldsymbol{x}_2^{\mathrm{T}}\boldsymbol{J}^{-1}\right\| \tag{42}$$

Theorem 3. *Consider a spacecraft described by Eq. (18), and the control laws are provided by Eqs. 41 and 42. When ω_d and $\dot{\boldsymbol{\omega}}_{\mathrm{d}}$ are all bounded, the following conclusions can be obtained.*

(1) $x_{1,i}$ converges to the region $|x_{1,i}| \leqslant \Delta_4$ and $x_{2,i}$ converges to zero in finite time T_1 where $\eta_1 = 2\min\{k_1,k_3\}$ and $\eta_2 = 2^{(\gamma+1)/2}\min\{k_2,k_4\,\beta^{(\gamma-1)/2}\}$.

$$T_1 \leqslant \frac{1}{\eta_1(1-\gamma)} \ln \frac{\eta_1 V_3(t_0)^{1-\gamma} + \eta_2}{\eta_2} \tag{43}$$

$$\Delta_4 = \eta \tag{44}$$

(2) The errors $\tilde{\boldsymbol{\omega}}$ converge to the regions $\|\tilde{\boldsymbol{\omega}}\| \leqslant \Delta_5$ in finite time.

$$\Delta_5 \leqslant k_1 \sqrt{\frac{8}{1+\cos\left(2\arcsin\left(\sqrt{3}\Delta_4\right)\right)}}\sqrt{3}\Delta_4 + k_2 \sqrt{\frac{8}{1+\cos\left(2\arcsin\left(\sqrt{3}\Delta_4\right)\right)}}\left(\sqrt{3}\Delta_4\right)^{\gamma} \tag{45}$$

(3) The region of attraction is given by $\boldsymbol{x}_1^{\mathrm{T}}(0)\boldsymbol{x}_1(0) + \frac{1}{\beta}\boldsymbol{x}_2^{\mathrm{T}}(0)\boldsymbol{x}_2(0) + \frac{1}{\chi}\tilde{d}_{\mathrm{M}}^2(0) < 1$.

The stability analysis of the controller Eqs. (41) and (42) is similar to Theorem 1 and Theorem 2.

4. Simulations

To validate the effectiveness of the proposed finite-time controllers, numerical simulations are given in this section. The proposed controllers are validated in the following scenario. The spacecraft is assumed to have available continuous actuators in three body axes with a maximum torque of 10 N·m. The spacecraft is required to track a common time-varying reference signal. For the dynamic model described by Eqs. (10) and (11), it should be noted that in the system there exist external disturbances with unknown bounds.

We design the continuous controller in the set υ, so it is not finite-time converging to the region near zero globally. From Theorem 2, we can know that the region of attraction is $\boldsymbol{x}_1^{\mathrm{T}}(0)\boldsymbol{x}_1(0) + \frac{1}{\beta}\boldsymbol{x}_2^{\mathrm{T}}(0)\boldsymbol{x}_2(0) + \tilde{\boldsymbol{d}}^{\mathrm{T}}(0)\boldsymbol{Q}^{-1}\tilde{\boldsymbol{d}}(0) < 1$. In order to illuminate that the region of attraction is large-angle, we choose $\boldsymbol{R}(0)$ equivalent to $\psi = 3.14$ rad, $\varphi = 2$ rad, $\theta = 1$ rad that is represented by Euler angles. $\boldsymbol{J}$ is the inertia matrix of the rigid spacecraft.

$$\boldsymbol{J} = \begin{bmatrix} 22.7 & 0.2 & -0.5 \\ 0.2 & 23.3 & 0.3 \\ -0.5 & 0.3 & 24.5 \end{bmatrix} \mathrm{kg}\cdot\mathrm{m}^2$$

$$\boldsymbol{R}(0) = \begin{bmatrix} -0.5415 & -0.7643 & 0.3502 \\ 0.0007 & 0.4161 & 0.9093 \\ -0.8407 & 0.4926 & -0.2248 \end{bmatrix}$$

$$\boldsymbol{\omega}(0) = [0.1\ 0.1\ 0.1]\ \mathrm{rad/s}$$

The expected attitude and velocity for the spacecraft and the disturbance torques $\boldsymbol{d}$ in the attitude dynamics Eq. (2) are defined as follows:

$$\boldsymbol{R}_{\mathrm{d}}(0) = \mathrm{diag}\ (1,1,1),$$

$$\boldsymbol{\omega}_{\mathrm{d}} = [0.1\sin(t/40) - 0.1\cos(t/50) - 0.1\sin(t/60)]^{\mathrm{T}}\mathrm{rad/s},$$

$$\boldsymbol{d} = 2\times10^{-3}[\sin(0.1t) - \cos(0.2t)\sin(0.2t)]^{\mathrm{T}}\mathrm{N}\cdot\mathrm{m}.$$

We select parameters of the first controller as $k_1 = 0.01$, $k_2 = 0.01$, $k_3 = 3$, $k_4 = 3$, $\gamma = 0.9$, $\beta = 10$, and $\boldsymbol{Q} = \mathrm{diag}\ (1,1,1)$. Simulation results of the spacecraft system under the controller Eq. (21) are shown in Figs. 1–5. In the figures, i represents the i th element of the corresponding vector. We can see that the attitude maneuver of the spacecraft can be

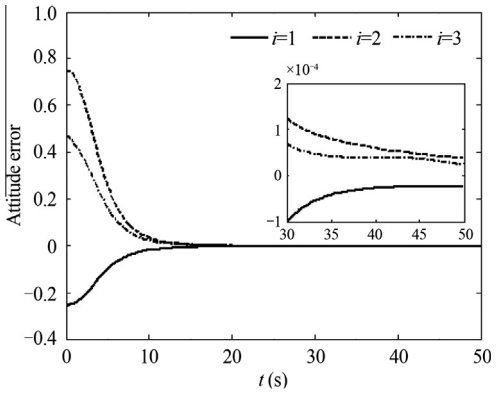

Fig. 1 Attitude curves of $\boldsymbol{e}_{\tilde{R}}$ under the first controller.

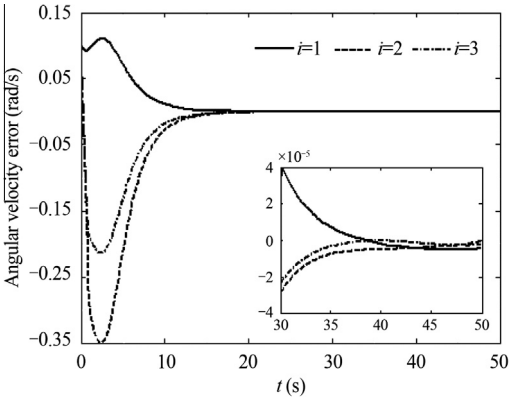

Fig. 2 Curves of angular velocity error $\tilde{\boldsymbol{\omega}}$ under the first controller.

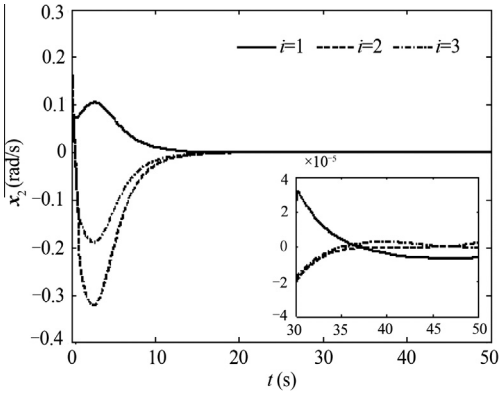

Fig. 3 Curves of tracking error $\boldsymbol{x}_2$ under the first controller.

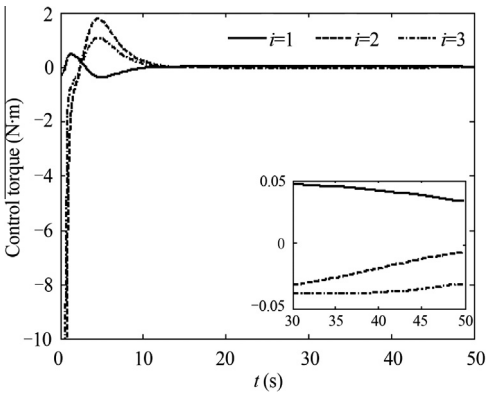

Fig. 4 Curves of control torque $\boldsymbol{u}$ under the first controller.

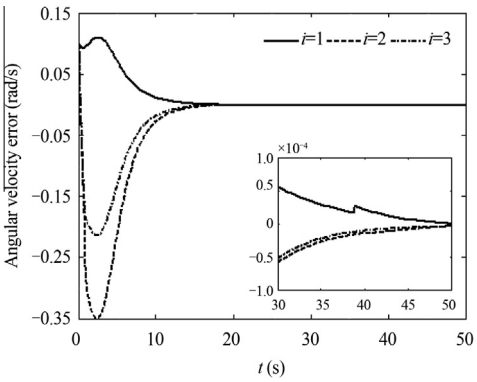

Fig. 7 Curves of angular velocity error $\tilde{\omega}$ under the second controller.

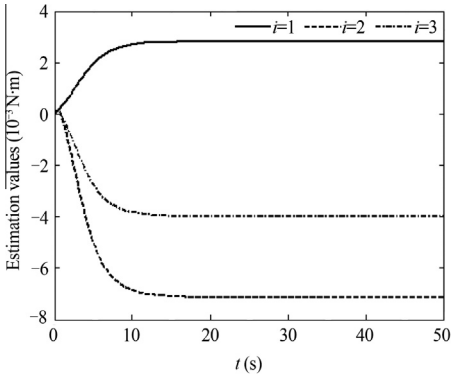

Fig. 5 Curves of estimated value $\hat{\boldsymbol{d}}$ under the first controller.

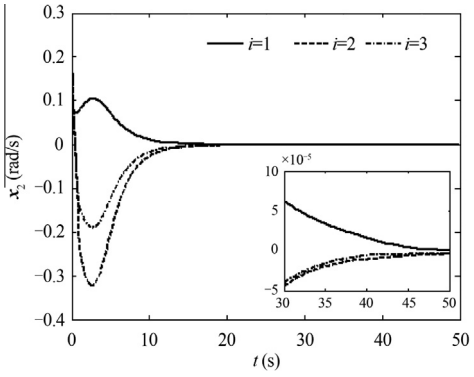

Fig. 8 Curves of tracking error $\boldsymbol{x}_2$ under the second controller.

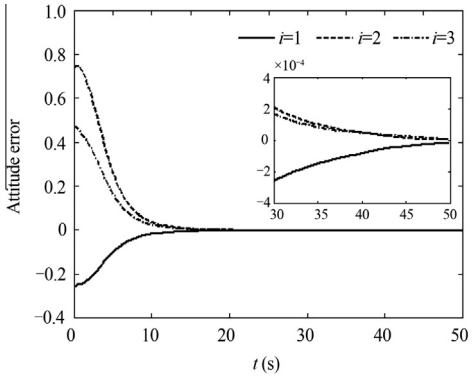

Fig. 6 Attitude curves of $\boldsymbol{e}_{\tilde{R}}$ under the second controller.

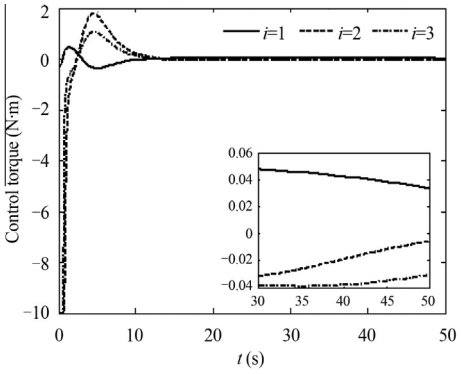

Fig. 9 Curves of control torque $\boldsymbol{u}$ under the second controller.

completed in less than 30 s. As the controller is continuous, it is free of chattering. Figs. 1–3 give the curves of $\boldsymbol{e}_{\tilde{R}}$, the angular velocity error $\tilde{\omega}$, and $\boldsymbol{x}_2$, respectively. Fig. 4 gives the curves of the control torque of the system, from which it can be seen that the maximum value of the control torque is 10 N·m. Fig. 5 gives the estimated value of the disturbance torque, from which it can be seen that the value of $\boldsymbol{d}$ can be estimated. From Figs. 1, 3 and 5, we can also see that the initialization satisfies the region of attraction. It is clearly seen that the controller Eq. (21) can obtain better performances when absolute attitude tracking is performed.

To validate the second controller, numerical simulations are given as follows. We select parameters of the second controller as $k_1 = 0.01$, $k_2 = 0.01$, $k_3 = 3$, $k_4 = 3$, $\gamma = 0.9$, $\beta = 10$, $\chi = 1$, $\lambda = 0.001$. In order to avoid chattering, we use saturation to take the place of sign function. Simulation results of the spacecraft system under the controller Eq. (41) are shown in Figs. 6–10. We can also see that the attitude maneuver of the spacecraft can be completed in less than 30 s.

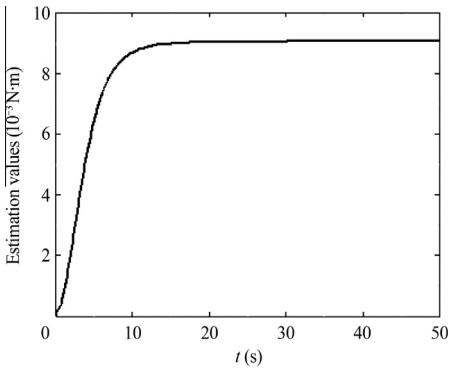

Fig. 10 Curves of estimated value $\hat{d}_M$ under the second controller.

5. Conclusions

(1) The primary contribution of this work is to develop two robust finite-time controllers based on rotation matrix for spacecraft. With the novel use of adaptive control, the second robust controller does not need the bounds of external disturbances.
(2) By the backstepping method and Lyapunov theorems, we get the overall closed-loop system is finite-time stable. Owing to external disturbances, the attitude error and the angular velocity error just converge to the region near zero in finite time.
(3) Simulations have shown that the continuous controller can make a spacecraft following a time-varying reference attitude signal without chattering in finite time and the discontinuous controller can also follow the signal.

Acknowledgements

The authors acknowledge the financial support provided by the National Natural Science Foundation of China (No. 61174037), the National Basic Research Program of China (973) (No. 2012CB821205, CAST20120602) and the National High Technology Research and Development Program of China (863) (No. 2012AA120602).

References

1. Wen JT, Kreutz DK. The attitude control problem. *IEEE Trans Automat Control* 1991;**36**(10):1148–62.
2. Sun HB, Li SH. Composite control method for stabilizing spacecraft attitude in terms of Rodrigues parameters. *Chin J Aeronaut* 2013;**26**(3):687–96.
3. Song SM, Zhang BQ, Wei XQ, Chen XL. Asymptotical stability analysis of "PD+" controller for spacecraft attitude tracking system. In: *Proceeding of the World Congress on Intelligent Control and Automation (WCICA)*; 2010. p. 3908–13.
4. Chaturvedi NA, Sanyal AK, McClamroch NH. Rigid-body attitude control. *Control System IEEE* 2011;**31**(3):30–51.
5. Bhat SP, Bernstein DS. A topological obstruction to continuous global stabilization of rotational motion and the unwinding phenomenon. *Syst Control Lett* 2000;**39**(1):63–70.
6. Chaturvedi NA, McClamroch NH, Bernstein DS. Asymptotic smooth stabilization of the inverted 3-D pendulum. *IEEE Trans Automat Control* 2009;**54**(6):1204–15.
7. Sanyal A, Fosbury A, Chaturvedi N, Bernstein D. Inertia-free spacecraft attitude tracking with disturbance rejection and almost global stabilization. *J Guid Control Dyn* 2009;**32**(4):1167–78.
8. Sarlette A, Sepulchre R, Leonard NE. Autonomous rigid body attitude synchronization. *Automatica* 2009;**45**(2):572–7.
9. Wang HL, Xie YC. On attitude synchronization of multiple rigid bodies with time delays. In: *Proceeding of the 18th IFAC World Congress*; 2011. p. 8774–9.
10. Lee TY. Exponential stability of an attitude tracking control system on SO(3) for large-angle rotational maneuvers. *Syst Control Lett* 2012;**61**(1):231–7.
11. Weiss A, Yang XB, Kolmanovsky I, Bernstein DS. Inertia-free spacecraft attitude control with reaction-wheel actuation. In: *Proceeding of AIAA Guidance, Navigation, and Control Conference*; 2010.
12. Cruz G, Yang XB, Weiss A, Kolmanovsky I, Bernstein DS. Torque-saturated, Inertia-free Spacecraft Attitude Control. In: *Proceeding of AIAA Guidance, Navigation, and Control Conference*; 2011.
13. Nersesov SG, Haddad WM, Qing H. Finite-time stabilization of nonlinear dynamical systems via control vector Lyapunov functions. *J Franklin Instit* 2008;**354**(7):819–37.
14. Hong YG, Xu YS, Huang J. Finite-time control for robot manipulators. *Syst Control Lett* 2002;**46**(4):243–5.
15. Bhat SP, Bernstein DS. Continuous finite-time stabilization of the translational and rotational double integrators. *IEEE Trans Automat Control* 1998;**43**(5):678–82.
16. Meng ZY, Ren W, You Z. Distributed finite-time attitude containment control for multiple rigid bodies. *Automatica* 2010;**46**(12):2092–9.
17. Du HB, Li SH. Finite-time attitude stabilization for a spacecraft using homogeneous method. *J Guid Control Dyn* 2012;**35**(3):740–8.
18. Yu SH, Yu XH, Shirinzadeh B, Man ZH. Continuous finite-time control for robotic manipulators with terminal sliding mode. *Automatica* 2005;**41**(11):1957–64.
19. Wu SN, Radice G, Gao YS, Sun ZW. Quaternion-based finite time control for spacecraft attitude tracking. *Acta Astronaut* 2011;**69**(1), 48-5.
20. Wang JY, Liang HZ, Sun ZW, Zhang SJ, Liu M. Finite-time control for spacecraft formation with dual-number-based description. *J Guid Control Dyn* 2012;**35**(3):950–62.
21. Reichhartinger M, Horn M. Finite-time stabilization by robust backstepping for a class of mechanical systems. In: *Proceeding of the IEEE International Conference on Control Applications*; 2011. p. 1403–9.
22. Zhang F, Duan GR. Robust integrated translation and rotation finite-time maneuver of a rigid spacecraft based on dual quaternion. In: *Proceeding of AIAA Guidance, Navigation, and Control Conference*; 2011.
23. Liu YC, Zhang T, Song JY, Liang B. Adaptive spacecraft attitude tracking controller design based on similar skew-symmetric structure. *Chin J Aeronaut* 2010;**23**(2):227–34.

Guo Yong received his B.S. degree in Control Science and Engineering from Harbin Institute of Technology in 2010. Currently, he is a Ph.D. student in the School of Astronautics at the same university. His main research interests include spacecraft coordination control and nonlinear control.

Song Shenmin received his Ph.D. degree in Control Theory and Application from Harbin Institute of Technology in 1996. He carried out postdoctoral research at Tokyo University from 2000 to 2002. He is currently a professor in the School of Astronautics at Harbin Institute of Technology. His main research interests include spacecraft guidance and control, intelligent control, and nonlinear theory and application.